SSC20-VI-04

Automated System Identification for Satellite Attitude Control

Hannah Weiher, Daniel Hernandez, Mitchel Craun, Evan Sperber, Alexander Harpenau, Carlos Beltran, Richard Chiang, Evan Ulrich
The Aerospace Corporation
2310 E. El Segundo Blvd., El Segundo, CA 90245; 310-336-5970
hannah.weiher@aero.org

ABSTRACT

A novel approach to on-obit system identification of satellite attitude control dynamics is presented. The approach is fully automated and will thus enable a variety of satellite applications, including high-performance proliferated constellations and modular payloads. The key enabling feature of the approach is the ability to estimate the uncertainty in the model and then perform additional data collections specifically to reduce the uncertainty. A prototype software implementation of the algorithm accurately estimated multiple structural modes in a CubeSat simulation and a CubeSat reaction wheel testbed in preparation for an on-orbit demonstration as part of the *The Aerospace Corporation's Slingshot 1* mission.

BACKGROUND

Like all control systems, a satellite attitude control system (ACS) is designed by trading stability and performance measures. System identification can thus be applied to improve the target system, or plant, model accuracy and reduce model uncertainty. These improvements in the plant model can then be used to improve control system performance by tailoring the controller to the plant or by reducing stability margins.

However, as in many other control system applications, the promise of system identification remains largely unfulfilled. Historically, a major obstacle to system identification in the satellite industry is that most satellites are very expensive, exquisitely designed systems that must meet requirements without relying on system identification since doing so complicates verification analyses. Thus, on-orbit system identification has typically only been used to verify structure modal frequencies. Additionally, the process has generally relied upon analysts on the ground to perform the identification on downlinked data and to direct iterative experiments. This process can be time consuming and costly when an entire ground crew needs to be staffed. Note that system identification in commercial terrestrial products has also been stymied by the need for a "person-in-the-loop", but rather because mass-produced products need to work reliably without any human intervention. The advent of proliferated constellations in low-Earth orbit (LEO) such as SpaceX's Starlink, presents similar opportunities and challenges.[1] The ACS for these relatively low-cost satellites must be robust to build-to-build variations and could benefit from system identification. Again, though, human involvement in the identification process is impractical. It is suggested here that many of these obstacles can be overcome by reliably automating system identification.

Previous satellite system identification efforts have established the viability of on-orbit identification by providing impressive results using a variety of model structures and fit techniques. For example, a Recursive Least Squares (RLS) filter, an Observer/Kalman filter identification (OKID) method, and a Box-Jenkins model have all been applied to on-orbit system identification. [2, 3, 4] However, none of the approaches provided a method for iteratively updating the excitation signal to refine the identified model. Additionally, while the results were compared to simulated and experimental data, only limited metrics such as prediction error sequence energy were provided for determining the reliability of the approach.

This work brings together known aspects of system identification theory to automate the system identification process and applies that process to a satellite ACS to improve performance and enable new concepts of operation. A key capability is the estimation of model uncertainties that are used to determine model quality and to determine experiment excitation signals while iteratively refining the model. These same model uncertainties can subsequently be used for controller synthesis or validation. Thus, automated system identification, when coupled with automated controller synthesis, enables shorter ACS design cycles and supports launching satellites more rapidly and efficiently by tuning the ACS on-orbit rather than the ground.

The autonomous system identification algorithms are currently being developed to be tested on-orbit on a payload called *Vertigo* which is planned for integration on The Aerospace Corporation's *Slingshot 1* CubeSat mission later this year. In this configuration, *Vertigo* will have its own dedicated set of sensors and actuators to command the desired response for the system identification algorithm as a stand-alone ACS payload in addition to the *Slingshot 1* primary ACS.

This paper first overviews the automated system identification approach and how it fits into a larger architecture involving automated controller synthesis. A discussion of the validation of the algorithms in simulation and on hardware, including results that compare favorably to analytical reference models, is then presented. The mathematical theory behind the automated system identification, the automated controller synthesis approach, and further applications of automated system identification will all be presented in future publications.

STRATEGY ARCHITECTURE

The processing flow for automated system identification and controller synthesis presented here, in Figure 1, is essentially the same process that any controls engineer would follow. The key enabler for automating the process is the computation of model uncertainties that are then used to drive the system identification and the controller design.

The Auto-Regressive Moving Average eXogenous input (ARMAX) model structure is used as it is a relatively simple model structure that allows for direct estimation of the plant and disturbance model parameters. In the ARMAX formulation, both the plant and disturbance processes are modeled as discrete time transfer functions as shown in Figure 2.

Given a sequence of experimentally collected input data $u(k)$ and output data $y(k)$, the estimate at the next time step $\hat{y}(k+1)$ is given by the following formula.[5]

$$\begin{aligned}\hat{y}(k) = &-a_1 y(k-1) - \cdots - a_{n_a} y(k-n_a) \; + \\ &b_1 u(k) + \cdots + b_{n_b} u(k-n_b+1) \; + \\ &c_1 e(k-1) + \cdots + c_{n_c} e(k-n_c)\end{aligned} \tag{1}$$

where the prediction error, $e(k)$, is defined as follows.

$$e(k) \equiv y(k) - \hat{y}(k) \tag{2}$$

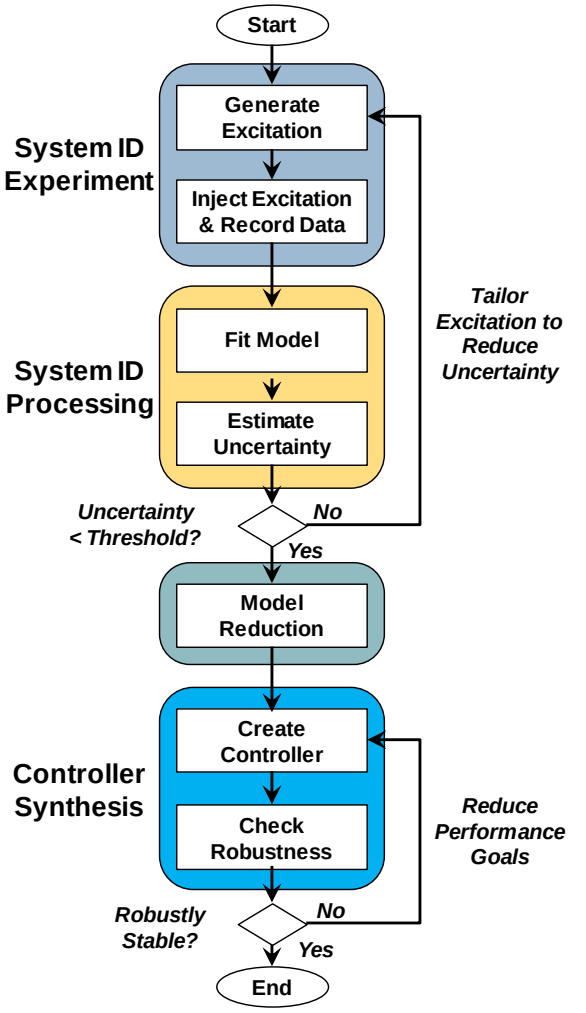

Figure 1: Automated System Identification and Controller Synthesis Processing Flow

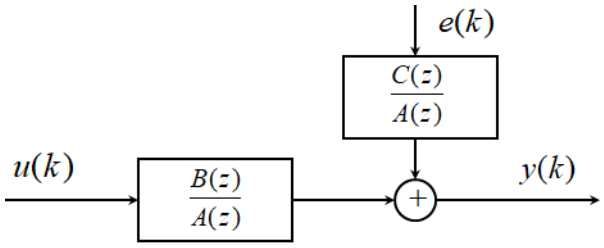

Figure 2: ARMAX Plant and Disturbance Models

The details for how the model fit is performed and how the frequency-dependent uncertainties are estimated will be provided in a future publication.

The initial system identification experiment uses additive white noise excitation since it is assumed that very little information on the plant is known a priori. An initial model is then fit to the data. Note that models that explicitly estimate the disturbance spectrum will tend to explain the data better. Quality checks specific to the model type may be performed. As an example, for prediction error models, the innovations, which are the disturbance inputs that are unexplained by the model, may be tested for whiteness or correlation with control inputs.

Estimated uncertainties of the plant frequency response and the disturbance spectrum are then computed. If the uncertainties are sufficiently small, then model reduction can optionally be performed on the model to improve numerical stability during controller synthesis. If they are not, then the frequency ranges with large uncertainties are determined and another system identification experiment is performed with energy only in those ranges. This process is repeated until the uncertainties are acceptably small across all frequencies of interest. While the model structure and estimation method are not specified, it is assumed that the system identification technique used supports computation of frequency response uncertainties and refinement of the model with additional data.

A straight forward way to limit excitation signal energy to a desired frequency range is to generate it as a chirp signal. This approach also facilitates avoiding known system nonlinearities such as actuator limitations by scaling the amplitude as a function of frequency.

Once the system identification iterations are complete, the estimated plant and disturbance model and the frequency-dependent plant and disturbance model uncertainties can be used for automated controller synthesis and stability analysis. The specifics of the controller synthesis and validation process will be detailed in a future publication.

The automated system identification process has been implemented first in MATLAB/Simulink and then as C code for embedded systems. As will be discussed in the Modeling and Simulation section, the code has been validated in a simulation of a CubeSat with inertial measurement unit (IMU) and reaction wheel assembly model parameters based on unit specifications. The code was then applied to a Reaction Wheel Testbed, as described in that section. In the coming year, on-orbit testing of the embedded code as part of the *Slingshot 1* flight software will raise the technology readiness level (TRL) from 4 (lab prototype) to 7 (space prototype).

MODELING AND SIMULATION

A detailed time domain simulation was developed using MATLAB Simulink for testing the behavior of the closed-loop system identification algorithm in a flight-like environment. This is valuable because it permits analysis of algorithm sensitivity to uncertain system characteristics such as sensor noise, physical geometry, and mass properties. A simulation also assists in design trades such as determining minimum reaction wheel sizes and torque limits.

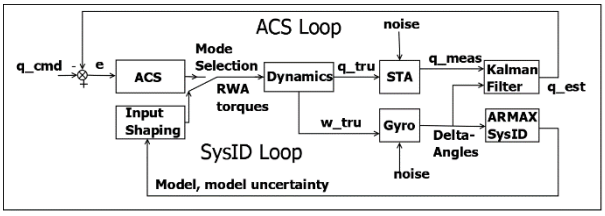

Figure 3: Time Domain Simulation Block Diagram

Space Vehicle Dynamics

The space vehicle is modeled as a multibody system with component rigid bodies connected at rigid interfaces or over stiff hinges. A demonstration platform is envisaged as a CubeSat-class mission and so the bus is sized using representative 12U mass properties. Deployed solar panels are modeled as uniform thin plates with "flex modes" approximated by applying torsional stiffness and damping at the interfaces. Since the first bending mode of the wing is expected to dominate, this investigation focuses on the attitude motion of the vehicle about the x-axis of the body frame (Figure 4).

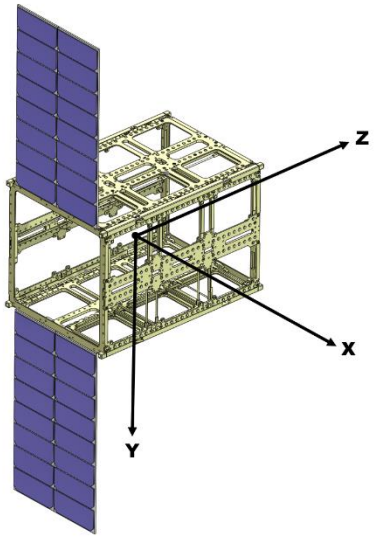

Figure 4: Bus Model

The bus model also contains three rigid single degree-of-freedom reaction wheels, one aligned with each body axis, to which attitude control torques can be applied in an equal and opposite sense relative to the bus mass. The nonlinear equations of motion are derived using Kane's Method facilitated by MotionGenesis. The equations of motion are extracted from the MotionGenesis simulation file and inserted into a Simulink Level 2 S-Function. The linearized dynamics (Figure 5) are computed using MATLAB's *linmod* and are included as a "truth" reference for the system identification algorithm.

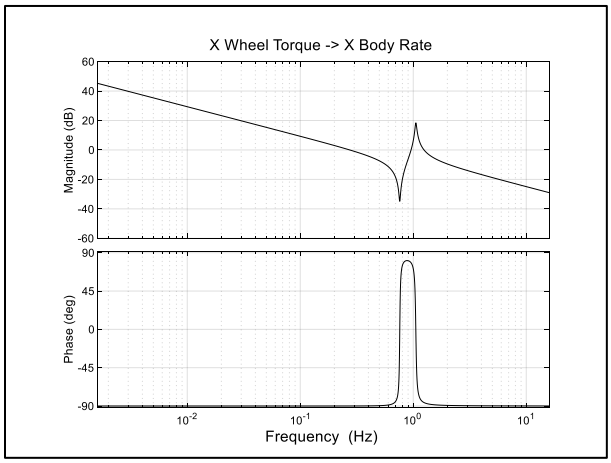

Figure 5: Linearized Dynamics Reference Model

Attitude Determination

The spacecraft ACS loop relies on both star tracker and gyro models providing input into a six state Kalman filter for estimating attitude. The system identification algorithms do not depend on the star tracker, so a low-fidelity model that simply adds noise to the truth attitude quaternions is used. The gyro outputs delta-angles which are inputs to the system identification routines; thus, special care is taken to ensure that the gyro model used in the simulation is high fidelity and includes realistic values for noise terms. To confirm the fidelity of the gyro model, laboratory gyro data was compared to simulated gyro data using an Allan Variance analysis to ensure a quality fit. The gyro being modeled is a commercial-off-the-shelf EPSON G364 unit.

System Identification Loop

A system identification state machine is implemented as a MATLAB script external to the time domain simulation. It drives the simulation by sitting in a loop and transitioning between states based on several criteria. While in the "experiment" state, torque commands are generated, and the simulation is run using the torque time series as reaction wheel inputs. Experiment substates include white noise experiments, log chirp experiments, and linear dwell experiments. While "processing," the model gyro output data is ingested, together with any previous model data, by the ARMAX algorithm and an updated model is obtained. New model uncertainty curves are also generated. The updated model and model uncertainty are used by the state machine to determine its next action. For example, it may generate a new input chirp signal centered at a detected mode or it may terminate the experiment if a sufficiently high-quality model has been obtained. The ACS loop remains open while the wheels are being commanded with the excitation inputs because the objective is to identify the open-loop plant dynamics. The system identification experiment could also be performed with closed-loop attitude control where the excitation input is added to the output of a low-bandwidth controller to stabilize the space vehicle attitude during the experiment.

SIMULATION RESULTS

A simulation case study was performed using an ARMAX model of order $n_a = n_b = n_c = 8$. As seen in Figure 6, the estimated model matches well with both the linearized analytical model and an empirical transfer function estimate (ETFE) based on power spectral density estimation. Note that both the estimated model and the ETFE indicate that there are high frequency dynamics not captured in the analytical model.

By design, the first two experiments run by the state machine use white noise and a logarithmically swept chirp as inputs, respectively. These broadband excitations help convergence of the backbone of the estimated model, with the white noise helping more at higher frequencies and the chirp at lower frequencies, but they typically leave large uncertainties near modes. Subsequently, a series of linear dwell-band chirps are computed centered at regions of high uncertainty which often correspond to modes.

The convergence of the model can be seen in Figure 7, which shows the reduction in weighted relative uncertainty in the frequency response. The weighting function is applied to prevent the algorithm from focusing on regions of high uncertainty in frequency bands that are not of interest. The reduction of the prediction errors, which is the goal of the optimization, is shown in Figure 8. In this case, the algorithm terminated when a maximum number of iterations was reached as the weighted relative uncertainty remained larger than the termination threshold of $-20\ dB$ at the 0.8 Hz anti-resonance. This uncertainty is acceptable for controller design and analysis since the loop gain is very small at that frequency.

Once an accurate model estimate has been obtained, model reduction techniques can be applied. The reduced

model can then be used for a host of applications such as parameter identification, control design, etc., all with a high degree of confidence.

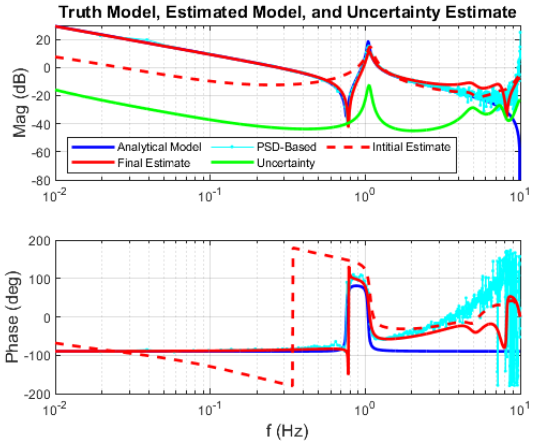

Figure 6: Simulated System Identification Results

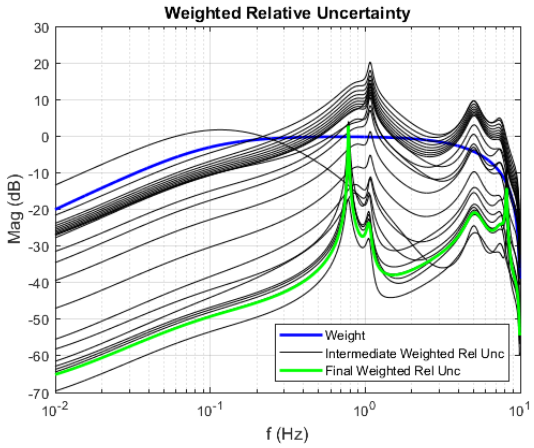

Figure 7: Convergence of Estimated Uncertainty

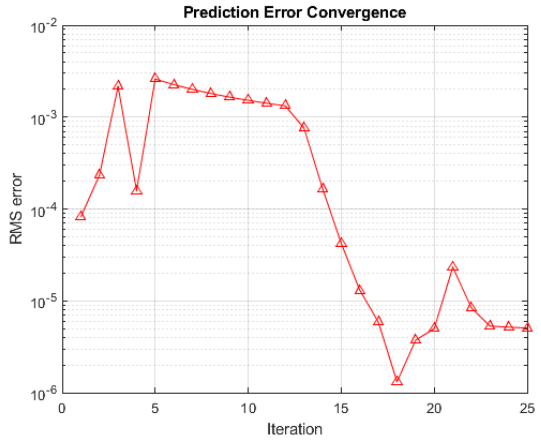

Figure 8: Convergence of Prediction Errors

With the state machine shown to work well in simulation, a hardware example is now discussed.

REACTION WHEEL TESTBED SETUP

The reaction wheel testbed was constructed to mimic a free-floating satellite in one dimension and provides the ability to test the algorithms using flight-like hardware.

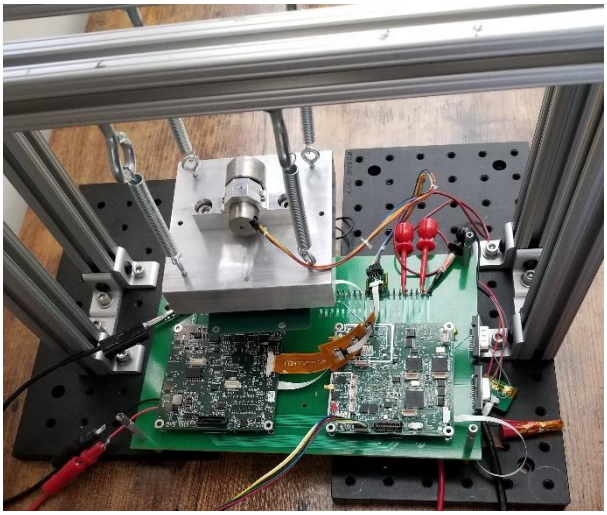

Figure 9: Reaction Wheel Testbed Setup Top View

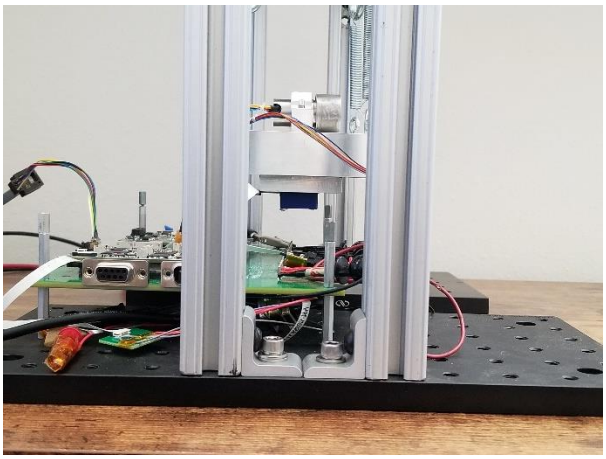

Figure 10: Reaction Wheel Testbed Setup Side View

The reaction wheel testbed consists of two crossbeams from which four helical springs are hung. This configuration results in two modes that are evident in the gyro measurements: a $\sim 6\ Hz$ "rocking" mode, and a $2\ Hz$ "pendulum" mode. All four springs are attached to an aluminum mass with a reaction wheel retention mechanism on the top and screw holes to fasten a gyroscope on the bottom. The green boards seen in Figure 9 host the electronics that acquire gyro data and send speed commands to the reaction wheel. The IMU is

again the EPSON G364 while the reaction wheels are made in-house.

The test is initiated by a host machine generating a reaction wheel command profile for a single axis from the automated system identification algorithm in MATLAB. The reaction wheel profile is then uploaded by custom Python ground software to flash memory embedded on engineering hardware, accessible by a micro-controller. The board support package, peripheral drivers and other application code are written in C. Upon upload and verification of a command profile, a 20 Hz control loop is started by the ground software. During each cycle of the control loop a reaction wheel command is read from flash storage and executed, and the measured gyroscope integrated angle and wheel speed are saved. At the end of the experiment iteration, the ground software downloads the integrated angles and measured wheel speeds from flash by serial communication. The system identification algorithm ingests the downloaded data and produces the next set of reaction wheel commands to be uploaded for the next iteration. The process ends once the weighted relative uncertainty falls below a specified threshold.

Since this algorithm is planned for integration on the *Vertigo* payload, using the verified MATLAB code with measured sensor data is an important incremental step to the future implementation of the automated algorithms on an embedded controller.

RESULTS

The results from applying the system identification approach to the reaction wheel testbed are shown in Figure 11 and Figure 12. In this case, the analytical frequency response is based on a first-principles physics model. The estimated model contains two significant modes within 20% of the predicted frequencies. However, damping ratios are harder to predict and the identified model shows that the peaking of the modes in the analytical model was significantly underestimated. Also, whereas the model has zero DC gain and thus predicts that the wheels must accelerate to produce an angular offset, the identified model suggests that there will be a small offset for nearly constant rates. This difference could be explained, for example, by misalignments between the input and output axes. Lastly, it is noted that while the estimated model can be used in controls analyses, the phase estimates of the ETFE based on the white noise experiment are too noisy to be used.

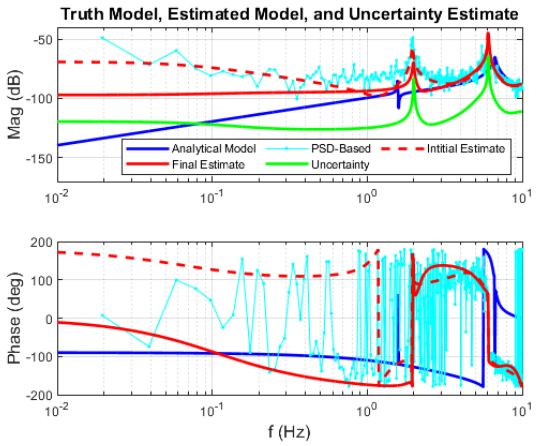

Figure 11: Convergence of Prediction Errors

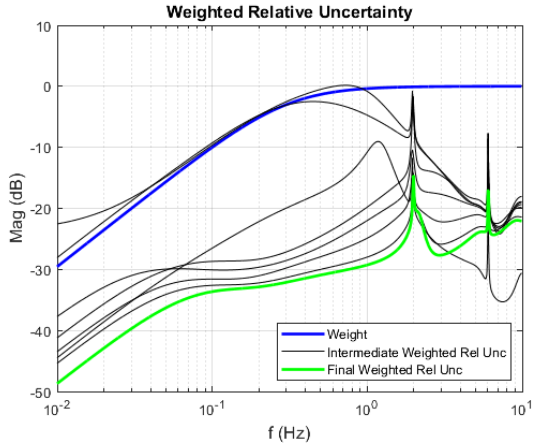

Figure 12: Convergence of Prediction Errors

DISCUSSION

This paper described the successful demonstration of an automated system identification algorithm. The algorithm was tested both in simulation and on hardware using a reaction wheel testbed. In simulation, the algorithm ran for several iterations, found a local minimum in a cost function, and terminated at the maximum number of iterations. The algorithm was run for fewer iterations on the reaction wheel testbed and still managed to produce a reasonably accurate model, although more iterations around the resonant frequencies would have improved the accuracy. During multiple runs of the algorithm in simulation and on the testbed, it was found that model convergence and accuracy depended strongly on model order selection. The model order is currently specified as an input to the algorithm, but it too could potentially be selected by the algorithm to obtain a higher quality model estimate. The reaction wheel testbed provided an initial test of the embedded process

by demonstrating the ability of the algorithm to identify more than one significant mode through the shaping of excitation signals in multiple regions of interest. The recursive nature of the system identification algorithm means the identification experiments in both simulation and hardware cases took minutes to hours in real time, whereas traditional system identification experiments may take an analyst days on the ground.

CONCLUSION

The automated system identification method presented in this paper enables more efficient use of time and resources by eliminating the need for a "person-in-the-loop". By automating this process, ACS design cycle timelines and complexity are reduced, and satellites can launch more rapidly and efficiently. Both the simulation and hardware testbed demonstrated the ability to identify the targeted system using an ARMAX model and reduced the model uncertainty through tailored, automated excitation inputs. The results, however, were sensitive to model order selection, which should be determined automatically in future work.

The next step is to finish validating the C code implementation of the algorithm on embedded systems in preparation for on-orbit testing as a stand-alone ACS payload called *Vertigo*, which is slotted to fly on Aerospace's *Slingshot 1* mission. *Slingshot 1* takes advantage of modularity to enable payloads, and thus satellites, to be launched more frequently, making *Vertigo* an ideal experimental candidate. Future plans also include implementing the model reduction algorithm and continuing research into automated controller synthesis that leverages the results from the automated system identification algorithm. These topics will be subjects of future publications.

ACKNOWLEDGMENTS

The authors would like to thank Farheen Rizvi (Control Analysis Department, *The Aerospace Corporation*) for her feedback on this paper as well as *The Aerospace Corporation's* iLab team for their support on this project.

REFERENCES

1. McDowell, J.C., "The Low Earth Orbit Satellite Population and Impacts of the SpaceX Starlink Constellation," Astrophysical Journal Letters, vol. 892, No. 2, April 2020.
2. Ghasemi, A., Moradi, M., and Ghasemi, H., "Modeling and System Identification of satellite," Proceedings of the 2nd International Conference on Control, Instrumentation and Automation, Shiraz, Iran, December 2011.
3. Li, W., Wang, D., and Liu, C., "System Identification of Large Flexible Appendage on Satellite for Autonomous Control," Proceedings of the 10th IEEE International Conference on Control and Automation, Hangzhou, China, June 2013.
4. Joshi, A., and Kim, W.-J., "System Identification and Multivariable Control Design for a Satellite UltraQuiet Isolation Technology Experiment (SUITE)," European Journal of Control, vol. 10, No. 2, 2004.
5. Keesman, K.J., System Identification: An Introduction, Springer-Verlag, London, 2011.